Petroleum Science 23 (2026) 2574–2586

Contents lists available at ScienceDirect

Petroleum Science

journal homepage: www.keaipublishing.com/en/journals/petroleum-science

Original Paper

Kerogen aromatization and late hydrocarbon generation: Evidence from position-specific isotope composition of propane

Feng-Jiao Li [a], Peng Liu [b], Wei-Wei Yang [c,d], Fu-Qi Li [e], Qian-Ping Wang [c,d], Ming-Yang Ma [a], Wen-Hui Liu [a], Dong-Dong Zhang [a,*], Xiao-Feng Wang [a,**]

[a] State Key Laboratory of Continental Evolution and Early Life, Department of Geology, Northwest University, Xi'an 710069, Shaanxi, China
[b] College of Safety Science and Engineering, Xi'an University of Science and Technology, Xi'an 710054, Shaanxi, China
[c] Research Institute of Exploration and Development, PetroChina Changqing Oilfield Company, Xi'an 710018, Shaanxi, China
[d] National Engineering Laboratory for Exploration and Development of Low Permeability Oil and Gas Fields, Xi'an 710018, Shaanxi, China
[e] Natural Gas Research Institute Branch, Shaanxi Yanchang Petroleum (Group) Co., Ltd., Xi'an 710061, Shaanxi, China

ARTICLE INFO

Article history:
Received 23 April 2025
Received in revised form
13 November 2025
Accepted 16 January 2026
Available online 22 January 2026

Edited by Min Li

Keywords:
Position-specific carbon isotope
Propane
Aromatization
Longdong area
the Ordos Basin

ABSTRACT

Natural gas accumulation involves complex multi-source mixing and post-genetic alterations that can lead to carbon isotopic reversals. Here, we report for the first time the co-occurrence of bulk and propane position-specific (PS) isotope reversals in conventional overmature gas reservoirs. We propose an aromatization-stabilization mechanism to explain these anomalous isotopic patterns. The Longdong area of the Ordos Basin provides a unique natural laboratory due to its well-defined thermal maturity gradient, the presence of multiple source rocks, and the coexistence of gases derived from different kerogen types. Integrated geochemical analyses of Cambrian-Carboniferous gases from six wells, reveal two key findings. First, the natural gases are in the overmature stage and exhibit both bulk carbon isotope reversals ($\delta^{13}C_1 > \delta^{13}C_2 > \delta^{13}C_3$ or $\delta^{13}C_1 > \delta^{13}C_2 < \delta^{13}C_3$), and Position-specific carbon isotope of propane anomalies ($\Delta_{C\text{-}T} = \delta^{13}C_{center} - \delta^{13}C_{terminal} < 0‰$; $\delta^{13}C_{center}$: isotopic composition of the central carbon in propane, $\delta^{13}C_{terminal}$: isotopic composition of the terminal carbon in propane). The propane in natural gas exhibits 25%–50% contribution from the isopropyl pathway. This is a formation mechanism theoretically restricted to low-maturity systems. This indicates preservation of early-formed branched precursors through cyclization/aromatization processes. We establish an "early-aromatization, delayed-cracking" model. This work highlights position-specific isotope analysis as a powerful tool for identifying post-genetic modifications in deep conventional and unconventional reservoirs.

1. Introduction

Hydrocarbon gases, recognized as one of the geological fluids present within the Earth's crust, are categorized into biogenic, thermogenic, and abiogenic origins (Dai et al., 2005, 2009, 2014b; Gold and Soter, 1980; Sherwood et al., 2002, 2006; Welhan and Craig, 1979). The precise determination of natural gas origins directly impacts resource assessment accuracy and exploration target selection. Hydrocarbon deposits of biogenic origins are generally identified by a positive sequence of carbon isotope compositions of alkanes, which is, $\delta^{13}C_1 < \delta^{13}C_2 < \delta^{13}C_3$ (Dai et al., 2014a; Schoell, 1980). However, natural gases generated from type I/II kerogen during the high-overmature stage often show a reversed isotope sequence (Dai et al., 2014b; Liu et al., 2015, 2016; Tilley and Muehlenbachs, 2013; Zumberge et al., 2012). Multiple mechanisms have been proposed to explain this phenomenon, primarily including gas mixing from different sources, microbial activity, thermochemical sulfate reduction (TSR), and water dissolution (Cheng et al., 2020; Dai et al., 2014b; Liu et al., 2018a; Song et al., 2021; Xia et al., 2013). Recent investigations of natural gas genesis in the Norwegian North Sea have increasingly recognized the influence of aromatization on carbon isotopic reversals. Closed-system pyrolysis experiments have documented carbon

* Corresponding author.
** Corresponding author.
E-mail addresses: zhangdd@nwu.edu.cn (D.-D. Zhang), wangxf@nwu.edu.cn (X.-F. Wang).
Peer review under the responsibility of China University of Petroleum (Beijing).

https://doi.org/10.1016/j.petsci.2026.01.024

isotopic variations in methane during aromatization processes (Dieckmann et al., 2006). Similarly, methylbenzene cracking experiments at 450 °C have demonstrated carbon isotopic reversals in alkane gases (Peng et al., 2020).

Previous experimental studies have successfully replicated potential aromatization pathways and shown that subsequent cracking of aromatization products may lead to reversed molecular carbon isotopic sequences (Dieckmann et al., 2006; Peng et al., 2020). However, the specific conditions required for aromatization remain unverified, as laboratory conditions cannot fully replicate the isotopic evolution trends observed during natural aromatization processes. Furthermore, molecular carbon isotopic signatures of natural gas components alone cannot adequately constrain the reaction mechanisms or formation pathways of aromatization processes. The position-specific (PS) carbon isotope composition analysis studies the stable isotope composition of atoms within different functional groups in a given organic molecule. Propane, the simplest alkane molecule containing non-equivalent carbon atoms in natural gas, has garnered significant attention in research (Galimov, 2006). PS isotopes of propane can reflect its formation pathways, reveal the chemical structure of precursor kerogen, and identify post-generation alterations (Liu et al., 2023a, 2024, 2025a; Wang et al., 2024). Consequently, the application of propane position-specific isotopes for tracing aromatization signatures becomes feasible. Various methods have been developed to determine PS isotopic distributions within propane (Gao et al., 2016; Gilbert et al., 2016; Liu et al., 2018b; Piasecki et al., 2018). Distinct reaction pathways involved in the formation of propane can result in $\delta^{13}C_{central} < \delta^{13}C_{terminal}$ at early stages of maturation, which shift to $\delta^{13}C_{central} > \delta^{13}C_{terminal}$ as maturation progresses. This intramolecular isotope rollover phenomenon has been documented in propane across various sedimentary basins (Liu et al., 2023a, 2024; Wang et al., 2024). Evidence from shale gas in the Wufeng Formation-Longmaxi Formation in south China supports the occurrence of intramolecular isotope re-rollover of propane during the high- and over-mature stages. This phenomenon can be attributed to surface-catalyzed abiotic polymerization of methane (C_1) as well as the inverse kinetic isotope effect (KIE) associated with hydrogen abstraction during the decomposition of ethane (C_2) and propane (Li et al., 2024; Shuai et al., 2023).

Current research indicates that aromatization processes may require catalytic cooperation between different kerogen types. The Longdong area in the Ordos Basin is uniquely suited for investigating aromatization processes under geological conditions. In the Longdong area, Upper Paleozoic source rocks dominated by Type III kerogen exhibit unconformable contact with Lower Paleozoic source rocks primarily composed of Type I/II kerogen. Critically, the contact zones between these source rocks, which contain Type I and II kerogens, create a natural interface, minimizing the complications from multiple gas charging events common in other basins.

This study provides the first documented evidence of concurrent bulk and intramolecular isotopic reversals in conventional gas reservoirs at post-maturity stages. By analyzing propane formation pathways and kinetic fractionation, we explore the primary causes of intramolecular carbon isotopic secondary rollover of propane in oil-type gas at a highly evolved stage. Our results demonstrate that aromatization-mediated preservation of early-maturity structural configurations constitutes the predominant mechanism responsible for both molecular and intramolecular carbon isotopic reversals. These findings provide valuable insights into the origins of natural gas in the Longdong area, southwest Ordos Basin.

2. Geological setting

The Ordos Basin is abundant in petroleum, natural gas, and coal reserves (Zhao et al., 2016) (Fig. 1(a)). Tectonic-sedimentary differentiation within the Ordos block became increasingly pronounced during the Cambrian period (Peng et al., 2023). In the central and western regions of the Ordos Basin, a north-south-trending central uplift was formed (Fig. 1(a)) (He et al., 2020, 2021). By the end of the Ordovician, the Ordos block experienced widespread uplift and erosion (He et al., 2021). As a result, the strata from the Upper Ordovician to the Lower Carboniferous are absent in the block, resulting in the regional unconformity between the Lower and Upper Paleozoic (He et al., 2021). During the sedimentation of the Taiyuan Formation, transgression expanded and encompassed the central paleo-uplift, creating a unified epicontinental sea sedimentary environment, with mudstone, shale, and carbonate rocks being the main deposits (Guo et al., 2014). In the southwest of the Ordos Basin, the Longdong area to the south of the central paleo-uplift, the Taiyuan Formation directly overlies the Cambrian Zhangxia Formation or the Jixian System (He et al., 2024; Huang et al., 2024) (Fig. 1(a)–(c)).

In the Ordos Basin, source strata comprise Upper Paleozoic and Lower Paleozoic (Ordovician and Cambrian) marine source rocks. In the Longdong area (southwestern basin; Fig. 1(b) and (c)), the Ordovician is absent, leaving two potential sets of source rocks: (1) Upper Paleozoic coal-measure source rocks, characterized by coal seams of 2–6 m thick and TOC up to 80%. Additionally, dark mudstone layers, with thicknesses between 10 and 80 m, exhibit TOC values of 0.5%–2.7% and R_o values of 2.0%–3.0%, indicating overmaturity (Sun et al., 2015; Yu et al., 2024). (2) Lower Cambrian black mudstone, with layers of 10–60 m thick, have TOC values varying between 0.4% and 11.0% and R_o values ranging from 2.4% to 4.9% (Huang et al., 2022, 2024; Liu et al., 2021), indicating overmaturity as well.

3. Materials and methods

3.1. Samples

Twelve natural gas samples were collected from northern basin (the Western Thrust Belt, R14; Tianhuan Depression, L50; Yishan Slope basin, YT1H 8.9, YT1H 7.9, J59-66 and Zh4) and Longdong area (L67, L68, L85, L54, L31, L43) within the Ordos Basin (Fig. 1) utilizing high-pressure vessels fitted with dual-valve systems. Prior to sampling, the high-pressure vessels were purged with natural gas to eliminate residual atmospheric components.

3.2. Chemical composition

The chemical composition of inorganic gases and hydrocarbons (C_1–C_5) was analyzed using a FULI 9790 Plus Gas Chromatograph (GC). Hydrocarbon components were separated using a capillary column coated with Al_2O_3 (30 m in length and 0.32 mm internal diameter), while inorganic gases were analyzed using a packed column containing a 5 Å molecular sieve (2.44 m in length and 3.15 mm internal diameter). The GC oven was programmed to an initial temperature of 60 °C, which was ramped to 290 °C at 4 °C/min and held for 15 min. A single injection allowed simultaneous detection of hydrocarbon and inorganic gases, achieved by precise control of 6-way and 10-way valve operations. The results are reported as volume percentages (%).

3.3. Compound-specific isotope composition

The compound-specific carbon isotope compositions of the associated gas samples were analyzed using a Thermo Scientific

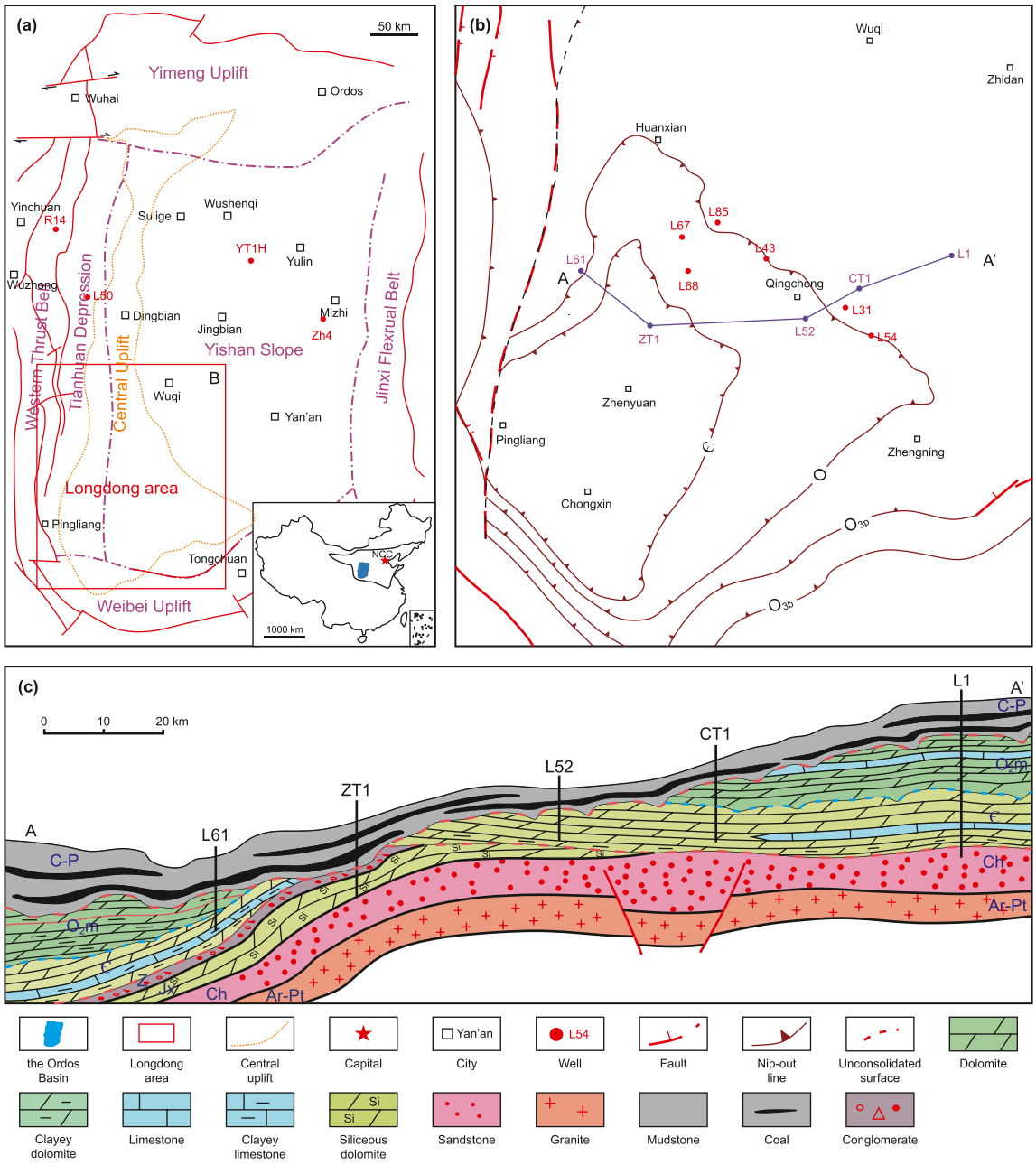

Fig. 1. (**a**) Location of the study area, (**b**) distribution map of the underlying strata of the Carboniferous System in the Longdong area and (**c**) stratigraphic section diagram of the Longdong area. NCC = North China Craton.

253 Plus Isotope Ratio Mass Spectrometer (IRMS) linked to a Thermo Scientific Trace 1310 Gas Chromatograph (GC). This GC is equipped with a capillary column (HP-PLOT Q). Initially, the GC oven was set to 30 °C and maintained for 10 min. Then, it was ramped up to 180 °C at a rate of 20 °C/min and held for 2 min. The $\delta^{13}C$ values were reported in per mil (‰) relative to the V-PDB standard, with an analytical precision of ±0.5‰.

3.4. PS carbon isotope composition of propane

The PS carbon isotope composition of propane analysis employed a q-NMR-calibrated GC-Py-GC-IRMS technique, as described in previous research (Liu et al., 2023a, 2023b, 2024, 2025b; Wang et al., 2024). Hydrocarbons in the gas samples were first separated by a primary GC column (HP-PLOT Q, 30 m × 0.32 mm inner diameter). The GC oven was initially set to 50 °C for 3 min, increased to 200 °C at 10 °C/min, and maintained at this temperature for 8 min. The separated hydrocarbons were then transported by high-purity helium to a pyrolysis reactor, consisting of a ceramic tube (50 cm in length and 0.7 mm inner diameter), maintained at a temperature of 790 °C. The resulting pyrolysis fragments were further separated using a secondary GC column (ZKAT-PLOT Q, 30 m × 0.32 mm inner diameter, 15 μm film thickness) with a constant oven temperature of 30 °C. These fragments are then transferred through a deactivated fused silica capillary column (with an internal diameter of 0.25 mm) to the combustion reactor of the GC-Isolink II, where the oxidation reaction is carried out at 1000 °C. The oxidation product (CO_2) is

carried to the Thermo Scientific MAT 253 Plus IRMS for $\delta^{13}C$ measurement. The integration of the GC columns, pyrolysis furnace, and mass spectrometer ensured precise determination of the carbon isotope compositions.

Previous studies have elucidated the origins of molecular fragments and the associated generation mechanisms involved in propane's thermal cracking. These investigations have demonstrated that methane and ethane are predominantly formed from the methyl group in propane, while ethylene production arises from an equal contribution of the methyl and methylene groups (Gilbert et al., 2016). $\Delta_{C\text{-}T}$ represents the proportion of contributions from methyl and methylene groups in propane. The PS isotopic composition of propane can be determined using the following approach:

$$\Delta_{C\text{-}T}\ (‰) = \delta^{13}C_{central} - \delta^{13}C_{terminal} \quad (1)$$

$$\delta^{13}C_{terminal} = \left(\delta^{13}C_{methane} \times S_{methane} + \delta^{13}C_{ethane} \times S_{ethane}\right) \Big/ \left(S_{methane} + S_{ethane}\right) \quad (2)$$

$$\delta^{13}C_{terminal} + {}_{\delta 13Ccentral} = 2 \times \delta^{13}C_{ethylene} \quad (3)$$

where $S_{methane}$ and S_{ethane} represent the area of CO_2 peak corresponding to methane and ethane, respectively. Using Eqs. (1)–(3), the $\Delta_{C\text{-}T}$ can then be determined.

4. Results

4.1. Gas compositions

The chemical compositions of natural gas from the Taiyuan Formation (C_2t) and Zhangxia Formation (ϵ_2zh) in the Ordos Basin are summarized in Table 1. Methane (C_1), ethane (C_2), and propane (C_3) are the predominant hydrocarbon components, with average concentrations of 78.06%, 2.20%, and 0.53%, respectively. The contents of Butane (C_4) and pentane (C_5) are relatively low, both below 0.1%. Inorganic gases are generally present at low levels. Notably, the sample from the L31 well exhibits elevated N_2 concentrations, reaching 64.51%. In other samples, N_2 content ranges from 1.33% to 20.62%, while CO_2 content varies from 0% to 7.21%.

4.2. Bulk isotopic compositions

The carbon isotope composition of natural gases derived from the Taiyuan Formation and Zhangxia Formation in the Ordos Basin does not exhibit distinct stratigraphic patterns typically associated with natural gas classification. Specifically, natural gases from both the Taiyuan and Zhangxia Formations in the Longdong area display comparable characteristics, and gases extracted from the Taiyuan Formation in other regions share similar attributes. Analysis of alkane gas carbon isotopes reveals two distinct trends with increasing carbon number (Table 2, Fig. 2). The first trend shows progressively heavier isotopic values with increasing carbon number, while the second displays an inversion of carbon isotopes. For these trends, the average $\delta^{13}C$ values in C_1, C_2, and C_3 are −33.67‰, −23.91‰, −22.93‰ (first trend) and −31.33‰, −34.59‰, −33.91‰ (second trend), respectively. Additionally, the average $\delta^{2}H$ values in C_1 are −183‰ and −176‰ for the two trends, respectively.

4.3. PS carbon isotope composition of propane

The PS carbon isotope composition of propane in natural gas samples from the Ordos Basin is presented in Table 3. The $\delta^{13}C$ values for the central and terminal carbon positions of propane ranged between −37.4‰ and −19.2‰, and between −36.2‰ and −21.2‰, respectively. Furthermore, both $\delta^{13}C_{central}$ and $\delta^{13}C_{terminal}$ display two distinct groups: one characterized by relatively heavier isotopic values and the other by relatively lighter values, consistent with the pattern observed in single-component carbon isotopes. In the Longdong area, the PS carbon isotope composition of propane is comparatively light, whereas that of propane from the northern basin within the Taiyuan Formation tends to be heavier. The $\Delta_{C\text{-}T}$ values vary widely, ranging from −2.7‰ to 3.8‰. In the Longdong area (L67, L68, L85, L54, and L43), propane samples exhibit negative $\Delta_{C\text{-}T}$ values from −2.7‰ to −0.7‰, suggesting that the $\delta^{13}C_{terminal}$ were heavier than $\delta^{13}C_{central}$. Conversely, in the northern basin (YT1H 8.9, YT1H 7.9, J59-66, Zh4, Li60, and R14), the $\Delta_{C\text{-}T}$ values are positive, ranging from 0.5‰ to 3.8‰, reflecting higher $\delta^{13}C_{central}$ relative to $\delta^{13}C_{terminal}$.

5. Discussion

5.1. Origins of the natural gases

Natural gas reservoirs form through a continuous supply of hydrocarbons from multiple sources under various geological processes (Xu, 1994). Stable isotopes of alkane gases serve as a key tool in tracing the origins of natural gas and determining genetic classification (Liu, 2015; Liu et al., 2007, , 2016, 2018c; Schoell, 1983; Xu et al., 2006). The relationship between $C_1/(C_2+C_3)$ and $\delta^{13}C_1$, as depicted in Bernard's plot, indicates a thermogenic origin for natural gases (Fig. 3). However, this relationship cannot differentiate kerogen types in thermogenic gases, necessitating further analysis using carbon isotopes of alkane gases.

Table 1
Chemical composition of natural gas from the Ordos Basin.

Group	Sample	Formation	Gas Compositions, %									
			CH_4	C_2H_6	C_3H_8	i-C_4H_{10}	n-C_4H_{10}	i-C_5H_{12}	n-C_5H_{12}	H_2	N_2	CO_2
Northern basin-C_2t	YT1H 8.9	C_2t	91.21	2.59	0.42	0.16	0.08	0.06	0.02	0.50	3.49	1.39
	YT1H 7.9	C_2t	74.33	2.13	0.34	0.12	0.06	0.04	0.02	0.80	20.62	1.49
	J59-66	C_2t	92.03	3.37	0.83	0.14	0.09	0.06	0.02	0.49	1.33	0.00
	Zh4	C_2t	95.55	2.16	0.44	0.06	0.04	0.00	0.02	0.16	0.41	0.00
	Li60	C_2t	84.31	2.62	0.29	0.05	0.03	0.00	0.02	0.38	10.54	1.71
	R14	C_2t	88.07	1.93	0.55	0.09	0.12	0.04	0.03	0.00	8.86	0.25
Longdong area-C_2t, ϵ_2zh	L67	C_2t, ϵ_2zh	82.39	2.87	0.54	0.07	0.08	0.03	0.01	0.17	6.57	7.21
	L68	C_2t	87.50	3.37	1.03	0.07	0.11	0.03	0.01	1.55	5.95	0.00
	L85	C_2t	90.44	3.54	0.90	0.08	0.08	0.02	0.04	0.00	2.10	0.00
	L54	C_2t	81.01	1.62	0.18	0.02	0.02	0.00	0.01	0.12	14.54	2.22
	L31	ϵ_2zh	19.67	0.10	0.03	0.00	0.00	0.00	0.00	1.45	64.51	10.96
	L43	ϵ_2zh	82.35	0.66	0.35	0.01	0.01	0.00	0.00	0.50	10.84	0.00

Table 2
Carbon and hydrogen isotopic compositions of alkane gas from the Ordos Basin.

Group	Sample	Formation	Carbon isotopic composition, ‰			hydrogen isotope composition, ‰
			CH_4	C_2H_6	C_3H_8	CH_4
Northern basin-C_2t	YT1H-8.9	C_2t	−33.4	−21.8	−20.6	−189
	YT1H-7.9	C_2t	−33.3	−21.8	−20.7	−188
	J59-66	C_2t	−34.2	−22.7	−22.0	−186
	Zh4	C_2t	−33.4	−24.1	−23.7	−178
	Li60	C_2t	−33.7	−23.3	−25.6	−192
	R14	C_2t	−34.1	−29.2	−27.7	−179
Longdong area-C_2t, ϵ_2zh	L67	C_2t, ϵ_2zh	−27.7	−32.9	−33.5	−187
	L68	C_2t	−30.8	−33.6	−33.9	−178
	L85	C_2t	−29.5	−35.0	−35.3	−179
	L54	C_2t	−31.8	−36.7	−36.6	−175
	L31	ϵ_2zh	−35.3	−32.6	−31.1	−169
	L43	ϵ_2zh	−32.9	−36.8	−33.0	−169

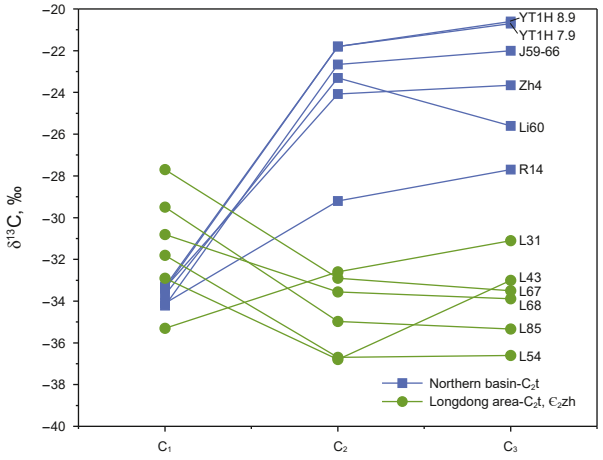

Fig. 2. $\delta^{13}C$ values of C_1–C_3 in the natural gases of the Taiyuan and Zhangxia Formation, the Ordos Basin. The squares are natural gas from the Taiyuan Formation in the northern basin, and the dots are natural gas from the Longdong area.

The Ro values of the source rocks were estimated using the empirical $\delta^{13}C_1$-R_o correlation established by Chen et al. (2021). For coal-type gas in the Taiyuan Formation in the northern part of the Ordos Basin, the average R_o value of source rocks is 1.1%, indicating a late mature stage, consistent with pyrolysis parameters of source rocks (Zhang et al., 2023). In the Longdong area, the average R_o value of source rocks for natural gas is 2.9%, representing an over-mature stage. However, the source rocks in this region have reached an over-mature stage with R_o values of 3.4% (Huang et al., 2022, 2024).

Carbon isotopes of alkane gases are effective indicators for distinguishing coal-type and oil-type gases. Typically, oil-type gas is characterized by $\delta^{13}C_2$ values below −28‰ and $\delta^{13}C_3$ values below −25‰, which are notably lower than those observed in coal-type gas. According to the $\delta^{13}C_1$ versus $\delta^{13}C_2$ classification diagram (Fig. 4(a)), natural gases in the Longdong area exhibit oil-type gas characteristics, while those from the Taiyuan Formation in the northern basin display typical coal-type gas features. Simultaneously, the $\delta^{13}C_2$ and $\delta^{13}C_3$ in Longdong natural gases are relatively light. Comparison with isotopic distribution curves derived from kinetic fractionation during thermal simulation experiments of different kerogen types indicates that the ethane and propane isotopes of Longdong natural gases plot within the low maturity stage (R_o < 0.6%–1.0%) of Type II kerogen (Fig. 4(b)). Most natural gas samples from the Taiyuan Formation in the northern basin are identified as coal-type gases, originating from type III kerogens. Their $\delta^{13}C_2$ and $\delta^{13}C_3$ align with the cracking model of Type III kerogen at a maturity range of R_o = 1.0%–1.6% (Fig. 4(b)), consistent with the thermal evolution level of the Taiyuan Formation source rocks (Zhang et al., 2023). Notably, samples from R14 exhibit oil-type gas, which may be related to Ordovician natural gas in the western margin of the basin (not discussed here). In contrast, the carbon isotopic composition of C_2 and C_3 in the natural gases in the Longdong region indicates parent materials originated from type I/II kerogens (Fig. 4(b)).

The carbon and hydrogen isotope compositions of alkane are good indicators for identifying the genesis of natural gas (Liu et al., 2004; Wang et al., 2006). Considering factors such as maturity, water medium type, and organic matter type, according to the relationship between the $\delta^{13}C_2$ and δ^2H of C_1 in various basins in China, a natural gas parent material identification chart was

Table 3
PS isotope composition of C_3 in the Ordos Basin.

Group	Sample	Formation	PS carbon isotope composition, ‰			s.d.
			$\Delta_{C\text{-}T}$	$\delta^{13}C_{terminal}$	$\delta^{13}C_{central}$	
Northern basin-C_2t	YT1H-8.9	C_2t	1.9	−21.2	−19.3	0.09
	YT1H-7.9	C_2t	2.2	−21.4	−19.2	0.01
	J59-66	C_2t	2.5	−22.8	−20.3	0.07
	Zh4	C_2t	3.8	−25.0	−21.2	0.28
	Li60	C_2t	0.6	−25.8	−25.2	0.12
	R14	C_2t	0.5	−27.9	−27.4	0.11
Longdong area-C_2t, ϵ_2zh	L67	C_2t, ϵ_2zh	−1.4	−33.0	−34.4	0.23
	L68	C_2t	−1.7	−33.3	−35.1	0.12
	L85	C_2t	−2.7	−34.4	−37.1	0.02
	L54	C_2t	−1.8	−36.2	−37.4	0.64
	L31	ϵ_2zh	/	/	/	/
	L43	ϵ_2zh	−0.7	−32.8	−33.5	0.10

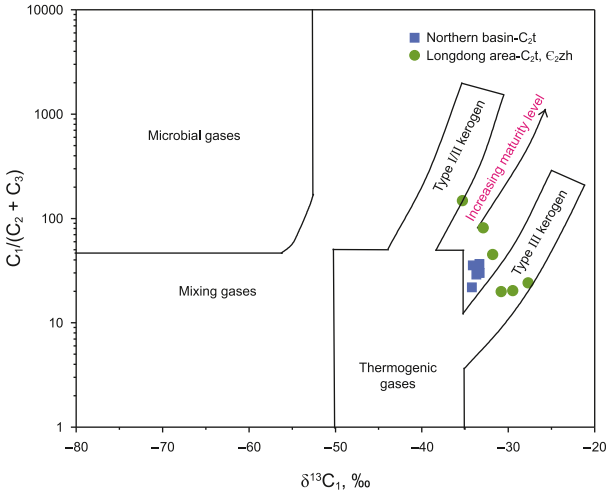

Fig. 3. The $C_1/(C_2+C_3)$ vs. $\delta^{13}C_1$ plot of the natural gases from the Ordos Basin (adapted from Bernard et al. (1978); Whiticar (1999)).

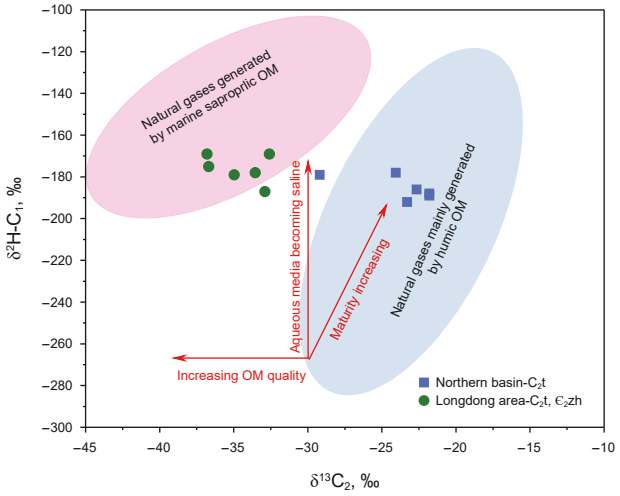

Fig. 5. Plot of $\delta^{13}C_2$ versus δ^2H-C_1 for natural gases of distinct genetic types (modified from Wang et al. (2015b)).

established to distinguish oil-type gas from coal-type gas (Fig. 5, Wang et al., 2015a, 2015b). The carbon isotope composition of C_2 and hydrogen isotope composition of C_1 (Fig. 5) yield consistent results as in Fig. 4. The natural gas samples from the Longdong area mainly fall within the region corresponding to natural gas derived from marine sapropelic organic matter, while other C_2t samples from the northern basin are typical of gas generated from humic organic matter.

The variations of $\delta^{13}C_{central}$ and $\delta^{13}C_{terminal}$ of propane in natural gases across multiple basins with diverse maturities are shown in Fig. 6. The $\delta^{13}C_{terminal}$ can assist in identifying the genesis of natural gas. The natural gas in the Taiyuan Formation exhibits the typical characteristics of type III kerogen. In the Longdong area, $\delta^{13}C_3$ values are approximately 11.5‰ lighter than those of coal-type gas in the Taiyuan Formation. Besides, $\delta^{13}C_{central}$ and $\delta^{13}C_{terminal}$ are 13.9‰ and 10.2‰ lighter, respectively, compared to coal-type gas in the Taiyuan Formation (Figs. 6 and 7), suggesting characteristics of type I/II kerogen.

The $\delta^{13}C_{central}$ of propane is significantly influenced by later-stage modification effects like microbial oxidation. Previous studies have proposed utilizing the regression slope between $\delta^{13}C_3$ and $\delta^{13}C_{central}$ to identify relationships with biological oxidation (Wang et al., 2024). Due to the selective modification of central carbon positions during biological oxidation, the slope between $\delta^{13}C_3$ and $\delta^{13}C_{central}$ (2.58) would be significantly greater than that resulting from alkane cracking (1.14). In the Longdong region, the observed slope between $\delta^{13}C_3$ and $\delta^{13}C_{central}$ is 1.10 (Fig. 7), which shows no evidence of substantial central carbon modification (Fig. 6). This finding effectively excludes significant post-generation alterations such as biological oxidation, supporting a predominantly thermal cracking origin for the propane in this system. Additionally, in highly evolved reservoirs, TSR represents a significant secondary alteration process responsible for carbon isotope inversion in natural gas composition sequences (Hao et al., 2008). High H_2S and CO_2 contents are key characteristics of TSR. However, no detectable H_2S content was identified in natural gas components from the Longdong area. Furthermore, as a secondary

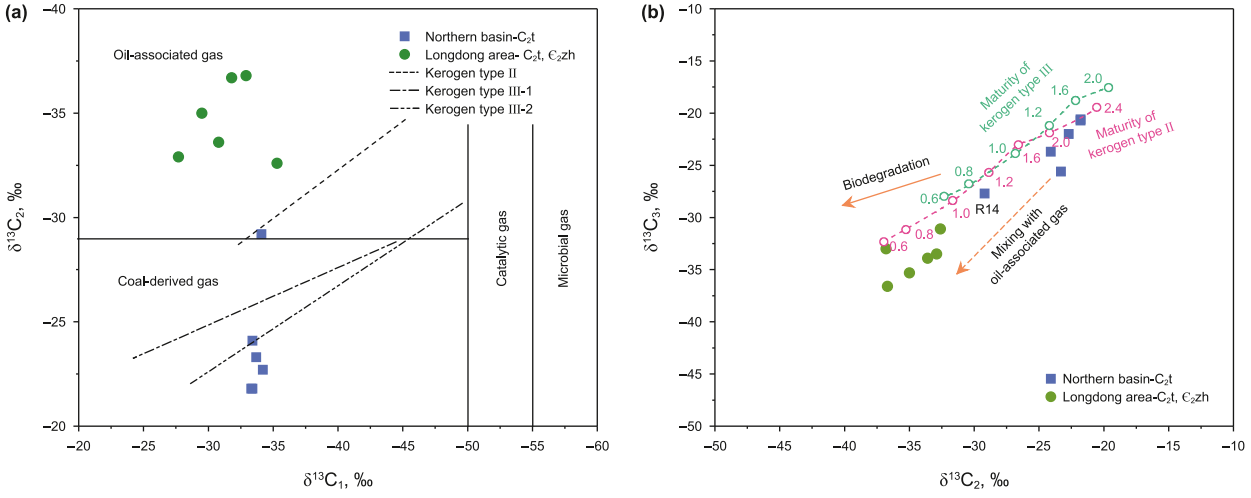

Fig. 4. Natural gas genesis discrimination diagram. **(a)** Cross correlation of $\delta^{13}C_1$ versus $\delta^{13}C_2$ for gases from the Ordos Basin (adapted from Sun and Huang (2004); the data of kerogen type II are from Delaware/Val Verde Basin, and the kerogen type III-2 are from Niger Delta, according to Rooney et al. (1995); the data of kerogen type III-1 are from Jenden et al., (1988); **(b)** Cross correlation of $\delta^{13}C_2$ versus $\delta^{13}C_3$ for natural gases of varying genetic types (adapted from Liu et al. (2018); isotope maturity model of kerogen type II and III is by Berner and Faber (1996); Etiope et al. (2014)).

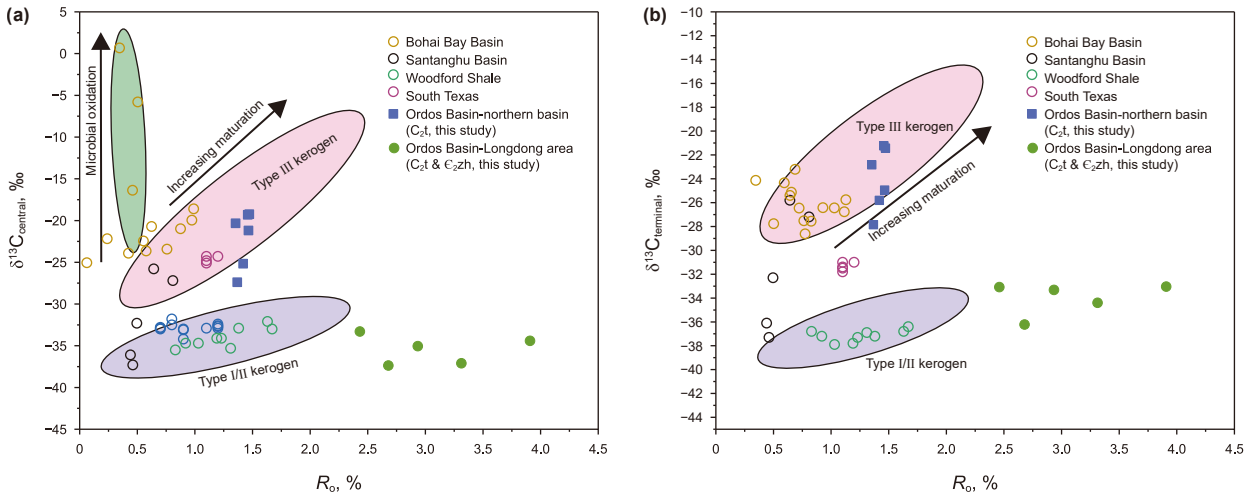

Fig. 6. Relationships between **(a)** $\delta^{13}C_{central}$ and **(b)** $\delta^{13}C_{terminal}$ with the maturity of the source rocks in natural gases from various basins. Data sources: Bohai Bay Basin (Wang et al., 2024); Santanghu Basin (Liu et al., 2024); Arkoma Basin (Liu et al., 2019b); Eagle Ford shale (Zhang et al., 2017; Zhao et al., 2020).

alteration process, TSR theoretically exhibits a selective effect on intermediate carbon isotope component of propane. Yet, this phenomenon was not observed. Therefore, the isotopic inversion is unrelated to secondary alteration processes.

Based on the molecular and isotopic compositions of natural gases in the Ordos basin, we conclude that the C_2t natural gas from the northern basin is typical thermogenic coal-type gas, while the Longdong area samples (C_2t, $€_2zh$) contain oil-type gas. In addition, the Taiyuan Formation of the northern part of the Ordos Basin, he characteristics of coal-type gas are consistent with the maturity of the source rocks. In contrast, in the Longdong area, the absolute values of carbon isotopes in the natural gas closely align with the distribution range characteristic of type I/II kerogen during the low-maturity stage.

5.2. Generation pathway of propane revealed by PS isotope analysis

Thermogenic propane has two pathways: the *n*-propyl (Pathway A) pathway and the isopropyl pathway (Pathway B) (Jin et al., 2024; Liu et al., 2023a). The energy barrier of the Pathway B is lower than that of the Pathway A (Hao et al., 2013; Liu et al., 2023a,2023b; Piasecki et al., 2018; Xia and Gao, 2024). However, some scholars argue that under geological conditions, the abundance of long-chain *n*-alkanes (which generate propane via Pathway A) is much higher than that of branched/isoprenoid compounds (which generate propane via Pathway B), so alkane cracking is dominated by the *n*-propyl pathway (Piasecki et al., 2018; Xia and Gao, 2024). This is supported by evidence from the Woodford Shale (R_o = 0.8%–1.7%) (Liu et al., 2019a, 2019b), as Type II kerogen is dominated by straight-chain aliphatic precursors. Nevertheless, Li et al. (2022) observed propane contributed by the isopropyl pathway at the low-maturity stage through thermal simulation experiments, and Jin et al. (2024) also confirmed that the structure of precursor substances affects the contribution of different pathways to propane formation via pyrolysis and simulation experiments.

Under ideal geological conditions (sufficient branched structures), propane formation preferentially occurs via Pathway B, which transitions to Pathway A as the reaction proceeds (Liu et al., 2023a,2023b). Additionally, a study on low-maturity natural propane in the Turpan-Hami Basin, 100% contribution from the

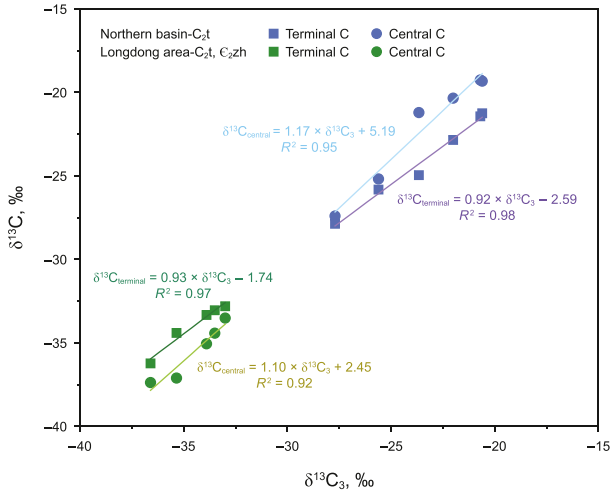

Fig. 7. Distribution map of $\delta^{13}C_3$ and specific positions isotopic compositions of propane in coal-type gas in the Taiyuan Formation of the Ordos Basin and in natural gas in the Longdong area.

isopropyl pathway was observed (Liu et al., 2023a, 2023b). Based on the relationship between isotope distribution and R_o, it is concluded that the decomposition of branched aliphatic chains at low maturity levels is of great significance for the formation of low-maturity natural gas (Liu et al., 2023a,2023b). In the *n*-propyl reaction pathway, isotopic kinetic fractionation mainly occurs at the terminal carbon, resulting in positive $\Delta_{C\text{-}T}$ values. Conversely, the isopropyl reaction pathway involves carbon-isotope fractionation mainly at the middle-position carbon, leading to negative $\Delta_{C\text{-}T}$ values. As a result, at the low-evolution stage, the central carbon isotope of propane is lighter than the terminal carbon isotope. However, as maturity increases, isopropyl in the kerogen structure is progressively consumed, and the reaction pathway shifts to the *n*-propyl pathway, which becomes the dominant route for propane generation. Consequently, $\Delta_{C\text{-}T}$ values of propane are negative in the early-maturity stage but become positive with increasing maturity (Liu et al., 2023a, 2024; Wang et al., 2024).

The natural gas in northern part of the basin (C_2t) shows positive $\Delta_{C\text{-}T}$ values, which is consistent with coal-type gas reservoirs observed in the remaining Ordos (Upper Paleozoic), Sichuan,

Tarim, and Bohai Bay Basins (Fig. 8(a)). Previous studies have calculated the intramolecular carbon isotope distribution in propane produced via varying proportions of *n*-propyl and isopropyl pathways in pyrolysis gas of different types of kerogens (Liu et al., 2024; Wang et al., 2024). The coal-type gas in the Taiyuan Formation demonstrates that propane is mainly derived from the *n*-propyl reaction pathway (Fig. 9). Furthermore, this gas also fits well with the kinetic models of n-C_{25} cracking (isothermal) and type III kerogen pyrolysis (heating), confirming its origin as typical thermogenic gas derived from type III kerogen (Fig. 9).

In the Longdong area, the $\Delta_{C\text{-}T}$ values are negative (Fig. 8(b)), indicating intramolecular carbon isotope inversion in propane at the high maturity stage. This phenomenon aligns with the kinetic processes typically observed in low maturity stages. Interestingly, this phenomenon has been first discovered in conventional gas reservoirs. Theoretical modeling of propane generation from type II kerogen via varying proportions of reaction paths (Fig. 10) shows 25%–75% of propane in the Longdong area is derived from the isopropyl pathway, further supporting the retention of early mature stage characteristics. Previously, such intramolecular carbon isotope inversion in propane with the increase of maturity, is exclusively found in unconventional gas reservoirs derived from Type I/II kerogen (Li et al., 2024; Shuai et al., 2023). Explanations for negative $\Delta_{C\text{-}T}$ values similar to those dominated by the isopropyl pathway in unconventional gas reservoirs include the polymerization of abiogenic methane (Li et al., 2024; Shuai et al., 2023) and hydrocarbon decomposition caused by hydrogen abstraction by kerogen surface radicals following inverse KIE (Xia and Gao, 2024).

The mismatch between natural gas characteristics and maturity indicates that the gas has undergone unique geological processes, consequently retaining the traits of low evolution despite reaching a high maturity stage. In the high evolution stage, kerogen pyrolysis generates gas, thereby releasing the information from the earlier low-evolution stage.

5.3. Intramolecular isotopic re-rollover caused by retention of hydrocarbon molecules at early maturation

Based on the above research on natural gas samples in the Longdong area, their intermolecular and intramolecular isotopic characteristics exhibit features typical of low-maturity oil-type gas. Notably, highly evolved natural gas in the Longdong area and shale gas in the Longmaxi Formation of the Sichuan Basin also exhibit negative $\Delta_{C\text{-}T}$ values of propane and lighter carbon isotope compositions at different positions, similar to those observed in the early stage (Li et al., 2024; Shuai et al., 2023; Xia and Gao, 2024). This indicates that certain characteristics of the low maturity stage are retained in these highly evolved natural gases.

The uniqueness of this study lies in the presence of a widespread weathering crust in the Longdong area, where marine and continental strata are in unconformable contact. Moreover, the natural gases from both sets of strata exhibit consistent geochemical characteristics, distinct from typical coal-type and oil-type gases. The presence of phenols and cycloalkane-aromatic ring systems in terrigenous Type III organic matter stabilizes aliphatic compounds in Type I kerogen through secondary reactions like ring-closure and aromatization (Dieckmann et al., 2006; Erdmann and Horsfield, 2006; Li et al., 2013; Muscio and Horsfield, 1996). This process requires contact between aliphatics

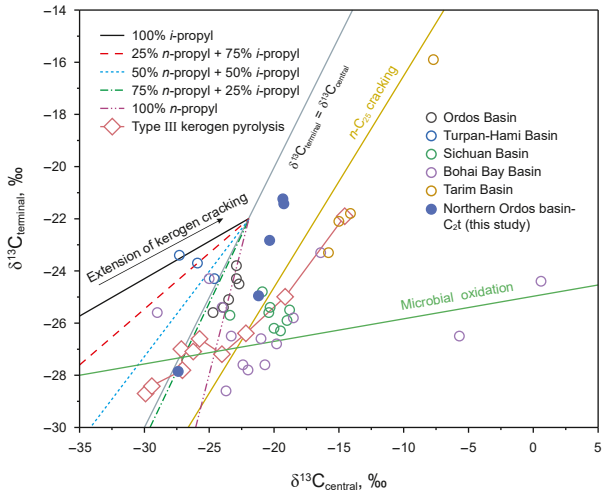

Fig. 9. Plot of $\delta^{13}C_{central}$ versus $\delta^{13}C_{terminal}$ of propane from kerogen cracking, modeled using the Rayleigh fractionation approach, and from natural samples. The linear tendency depicts the PS isotope composition of propane from the pyrolysis of type III kerogen (Zhang et al., 2022), while the trend for microbial oxidation is based on Gilbert et al. (2019). Data were sourced from Wang et al. (2024).

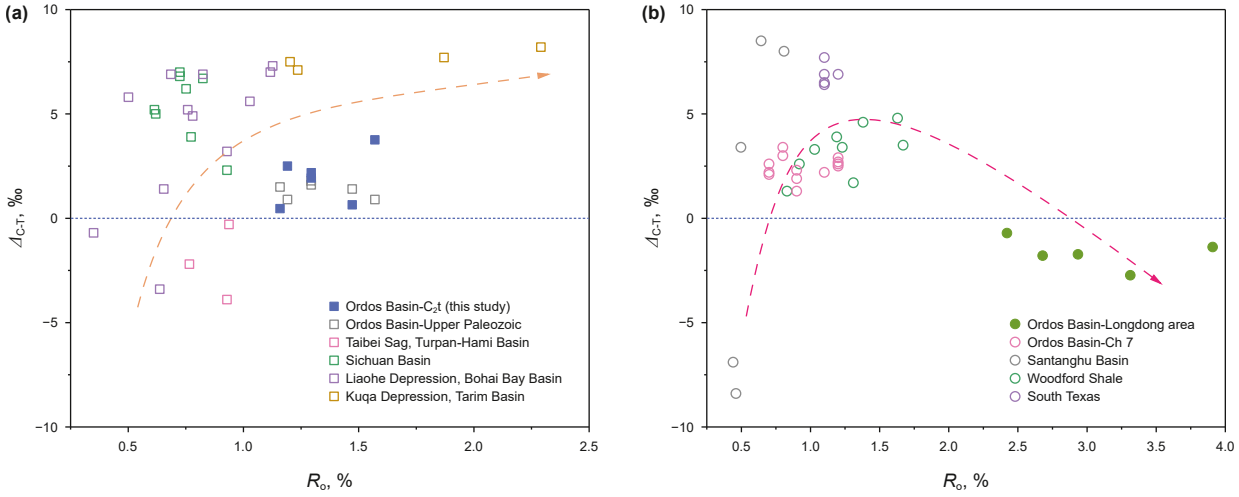

Fig. 8. Correlation between the $\Delta_{C\text{-}T}$ of C_3 and the R_o for natural gases derived from type III kerogen **(a)** and type I/II kerogen **(b)**. Data were sourced from the Ordos Basin, Turpan-Hami Basin, Sichuan Basin, Bohai Bay Basin, Tarim Basin, Santanghu Basin, Arkoma Basin, and South Texas (Liu et al., 2019a, 2023a, 2024; Wang et al., 2024; Zhao et al., 2020).

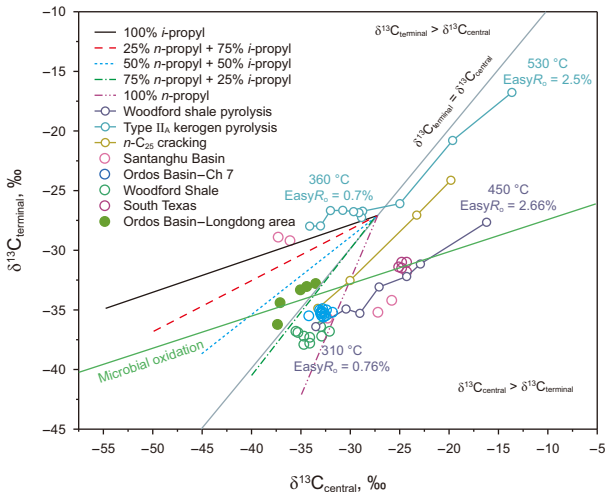

Fig. 10. Plot of $\delta^{13}C_{central}$ versus $\delta^{13}C_{terminal}$ of propane in natural gases from the Longdong area of the Ordos Basin, alongside accumulated propane generated during the thermal cracking of kerogen through various reaction pathways. Propane data from the Woodford Shale pyrolysis and Type II_A kerogen pyrolysis are derived (Li et al., 2022; Zhang et al., 2022). The trend line of n-C_{25} cracking was constructed with results from Gilbert et al. (2019). Data on propane from the Santanghu Basin, the Arkoma Basin, and South Texas were collected (Liu et al., 2019b, 2024; Zhao et al., 2020).

in Type I kerogen and aromatics in Type III kerogen. Owing to the presence of paleohighs in the Longdong area, the Lower Paleozoic source rocks dominated by Type I kerogen are in direct contact with the Upper Paleozoic coal-bearing source rocks dominated by Type III kerogen, providing favorable geological conditions for aromatization. During pyrolysis, aliphatic carbons in kerogen, such as alkyl chains, hydrogenated aromatic structures, and cycloalkanes, convert into aromatic hydrocarbons through dehydrogenation, where hydrogen is captured by free radicals (Dieckmann et al., 2006; Erdmann and Horsfield, 2006; Muscio and Horsfield, 1996). Aromatization occurs as a thermally stable process during the early maturation stage. This process effectively fixes the molecular structures and characteristics indicative of low maturity. Secondary recombination reactions during the low evolution stages allow hydrocarbons to retain abundant side-chain structures from the parent material during the cyclization and/or aromatization process (Fig. 11), such as the isotopically light signature characteristic of propane formed via the isopropyl pathway. Aromatized products are more thermally stable than primary kerogen and exhibit significant thermal hysteresis during cracking. This stability thereby increases their gas potential at high maturity (VR_o~2%) and high temperatures (>200 °C) (Dieckmann et al., 2006; Erdmann and Horsfield, 2006).

These stable configurations explain the negative $\Delta_{C\text{-}T}$ values and inverted carbon isotope patterns observed in the high evolution stages (Fig. 11). Liquid hydrocarbons are generated from the Lower Paleozoic source rocks in the Longdong area in the Longdong area during the low-maturity stage. After migration, these liquid hydrocarbons come into direct contact with Type III kerogen and underwent aromatization of early-stage hydrocarbons catalyzed by Type III kerogen or other factors, preserving low-maturity characteristics of ^{13}C-depletion and branched-chain structures. These characteristics subsequently influenced secondary gas generation at high maturity stages (Fig. 12), releasing the low-maturity signatures that were stabilized by prior aromatization

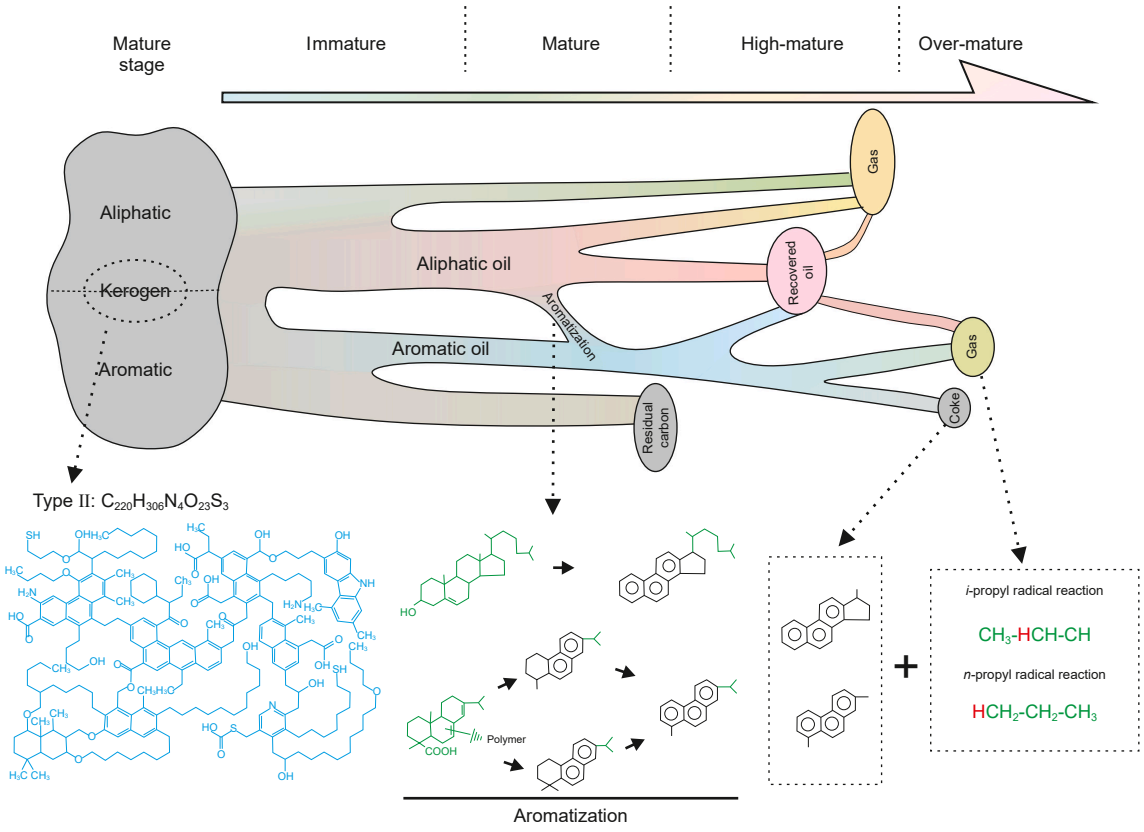

Fig. 11. Schematic diagram of the preservation of side chain alkyl groups by aromatization of type II kerogen (Huang et al., 2018) at the low maturity stage and the release of propane through different pathways at the high evolution stage.

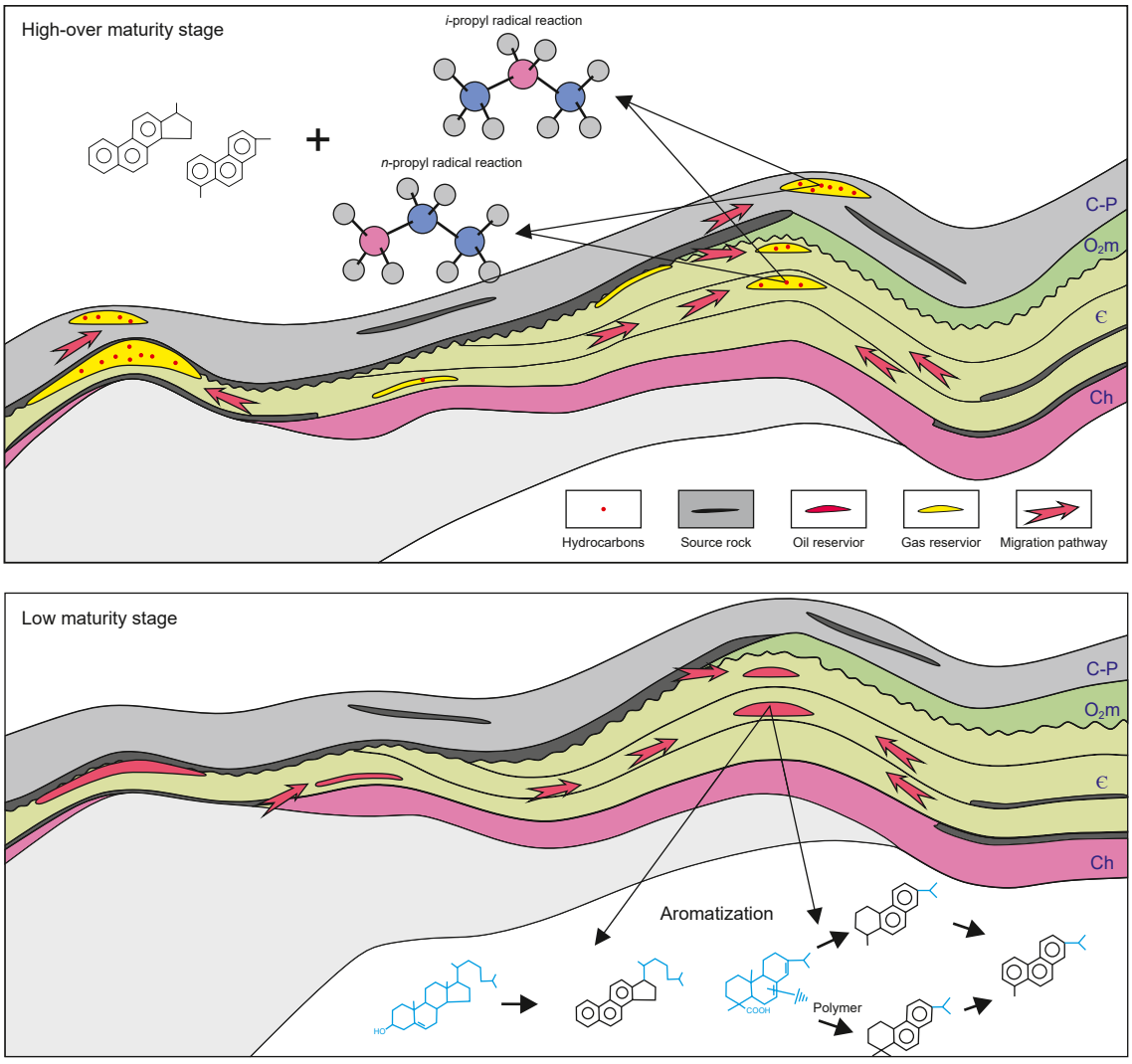

Fig. 12. Evolution pattern diagram of different stages of aromatization the natural gas migration in the Longdong area.

during the over-mature stage. Therefore, natural gas reservoirs contain two distinct genetic components: gases generated through conventional alkane cracking, and gases produced by the cracking of aromatization products at high to post-maturity stages. During conventional thermal maturation, methane derived from kerogen cracking becomes progressively enriched in ^{13}C with increasing thermal stress. Compared to the primary stage, methane from over-mature kerogen cracking is enriched in ^{13}C. Conversely, among aromatization products, the activation energies required for breaking methyl, ethyl, *n*-propyl, and isopropyl groups progressively decrease. At high to post-maturity stages, the thermally stable aromatization products begin to release early-formed branched structures that retain relatively higher ^{12}C contents. This delayed release of ^{12}C-enriched moieties ultimately leads to the observed carbon isotopic reversals.

5.4. Implications for gas source identification and geological significance

As discussed in Section 5.1, the reversed natural gas in the Longdong area is oil-type gas, sourced from the underlying marine strata rather than the Carboniferous-Permian coal-measure strata. The gas reservoir exhibits characteristics indicating that the source rock reached a R_o value of approximately 3.4%. Given that the maturity of the Ordovician source rocks (1.8%–2.8% at the top) is inconsistent with gas characteristics, the Longdong reservoir likely sourced from older, more mature strata such as Cambrian or Precambrian mudstones. Furthermore, due to the presence of the Qingyang paleo-uplift, the Ordovician are predominantly absent in the Longdong area (Figs. 1 and 12). Ordovician carbonate strata are distributed peripherally, with the Upper Ordovician Pingliang Formation shales developed only in the south. An Ordovician origin for the source rocks is considered unlikely. Therefore, the source rocks of this gas reservoir are likely the Cambrian and even older strata, such as Precambrian mudstone. Recent studies have confirmed the presence of Cambrian bitumen with R_o values of 1.35%–3.48% in the south of the Qingyang paleo-uplift (Huang et al., 2022, 2024). These Cambrian and Precambrian Jixianian system reservoir bitumen samples indicate exposure to high temperatures of 160–236 °C, sufficient to trigger the cracking of large amounts of aromatization products and the formation of significant amounts of natural gas (Fig. 12, Huang et al., 2022, 2024).

This research, through the innovative implementation of position - specific isotope analysis, propels the fundamental comprehension of carbon isotopic reversal phenomena within natural gas

systems. They thus offer a novel and robust perspective for gas source identification, supplementing the limitations of traditional bulk isotope methods. Notably, the detection of preserved low-maturity isotopic signatures in overmature gases contradicts existing models. It uncovers the crucial role of aromatization in retention the isotopic fingerprints from early-generation hydrocarbons during geological evolution. The proposed stabilization mechanism, which involves cyclization/aromatization, constructs a theoretical framework for interpreting anomalous isotope distributions in deep-seated petroleum reservoirs. Currently, we are employing molecular geochemical methods to investigate evidence of aromatization processes within source rocks. Our ultimate aim is to pinpoint the hydrocarbon origins and alteration processes of this gas reservoir to support exploration requirements.

6. Conclusions

This study employs position-specific isotope analysis of propane to conduct precise measurements of reversed natural gas in the Longdong area. By tracing the natural propane generation process, we elucidate how aromatization affects the position-specific isotope distribution of generated propane. The main conclusions are as follows:

1. In the Longdong area of the Ordos Basin, the natural gas exhibits bulk and intramolecular carbon isotopic reversals, distinct from typical coal-type gas, suggesting primarily derived from Type I/II kerogen.
2. The analysis of propane PS carbon isotopes reveals two primary generation pathways: the isopropyl pathway dominates at low maturity stages, while the *n*-propyl pathway becomes predominant at high maturity stages. The natural gas in the Longdong area retains isotopic characteristics of the low maturity stage, even at high maturity, indicating the preservation of early-generation hydrocarbons.
3. Early-generation characteristics are attributed to the stabilization of early-generated liquid hydrocarbons through cyclization and aromatization. This catalytic secondary reorganization of aliphatics by aromatics produces compounds more stable than kerogen. These stabilized compounds later released natural gas during high-temperature cracking, preserving the isotopic patterns of the early stage. The Longdong area provides an ideal natural setting for this reaction.
4. The natural gas in the Longdong area likely originates from ancient Cambrian or even Precambrian source rocks. The presence of large-scale ancient oil reservoirs in this region is inferred. The study underscores the importance of considering intramolecular isotopic variations for accurate gas source identification and contributes to understanding the hydrocarbon generation and preservation processes in highly evolved basins.

CRediT authorship contribution statement

Feng-Jiao Li: Writing – original draft, Visualization, Formal analysis. **Peng Liu:** Writing – review & editing, Validation, Methodology. **Wei-Wei Yang:** Resources. **Fu-Qi Li:** Methodology. **Qian-Ping Wang:** Resources. **Ming-Yang Ma:** Software, Methodology. **Wen-Hui Liu:** Supervision, Funding acquisition. **Dong-Dong Zhang:** Writing – review & editing, Supervision, Funding acquisition. **Xiao-Feng Wang:** Writing – review & editing, Project administration, Methodology.

Declaration of competing interest

The authors declare that they have no known competing financial interests or personal relationships that could have appeared to influence the work reported in this paper.

Acknowledgments

This work was financially supported by the National Natural Science Foundation of China (Grant No. 42230815); the Major Special Projects of Changqing Oilfield (Grant No. 2024D1JC06); and the Youth Innovation Team Project by Shaanxi Provincial Department of Education (No. 23JP173). The authors appreciated Dr. Xiao-Fu Li and Shao-Lin Zeng for their technical support with the use of the MAT 253 plus mass spectrometer.

Thank you to the Editor and the anonymous reviewers for their constructive comments on improving the quality of the manuscript.

References

Bernard, B.B., Brooks, J.M., Sackett, W.M., 1978. Light hydrocarbons in recent Texas continental shelf and slope sediments. Geophys. Res. Oceans 83, 4053–4061. https://doi.org/10.1029/JC083iC08p04053.

Berner, U., Faber, E., 1996. Empirical carbon isotope/maturity relationships for gases from algal kerogens and terrigenous organic matter, based on dry, open-system pyrolysis. Org. Geochem. 24, 947–955. https://doi.org/10.1016/S0146-6380(96)00090-3.

Chen, J., Wang, X., Chen, J., et al., 2021. New equation to decipher the relationship between carbon isotopic composition of methane and maturity of gas source rocks. Sci. China Earth Sci. 64, 470–493. https://doi.org/10.1007/s11430-020-9692-1.

Cheng, B., Xu, J., Deng, Q., et al., 2020. Methane cracking within shale rocks: A new explanation for carbon isotope reversal of shale gas. Mar. Petrol. Geol. 121, 104591. https://doi.org/10.1016/j.marpetgeo.2020.104591.

Dai, J., Zou, C., Liao, S., et al., 2014b. Geochemistry of the extremely high thermal maturity Longmaxi shale gas, southern Sichuan Basin. Org. Geochem. 74, 3–12. https://doi.org/10.1016/j.orggeochem.2014.01.018.

Dai, J., Yang, S., Chen, H., et al., 2005. Geochemistry and occurrence of inorganic gas accumulations in Chinese sedimentary basins. Org. Geochem. 36, 1664–1688. https://doi.org/10.1016/j.orggeochem.2005.08.007.

Dai, J., Ni, Y., Zou, C., et al., 2009. Stable carbon isotopes of alkane gases from the Xujiahe coal measures and implication for gas-source correlation in the Sichuan Basin, SW China. Org. Geochem. 40, 638–646. https://doi.org/10.1016/j.orggeochem.2009.01.012.

Dai, J., Yu, C., Huang, S., et al., 2014a. Geological and geochemical characteristics of large gas fields in China. Petrol. Explor. Dev. 41, 1–13. https://doi.org/10.1016/S1876-3804(14)60001-X.

Dieckmann, V., Ondrak, R., Cramer, B., et al., 2006. Deep basin gas: New insights from kinetic modeling and isotopic fractionation in deep-formed gas precursors. Mar. Petrol. Geol. 23, 183–199. https://doi.org/10.1016/j.marpetgeo.2005.08.002.

Erdmann, M., Horsfield, B., 2006. Enhanced late gas generation potential of petroleum source rocks via recombination reactions: Evidence from the Norwegian North Sea. Geochem. Cosmochim. Acta 70, 3943–3956. https://doi.org/10.1016/j.gca.2006.04.003.

Etiope, G., Panieri, G., Fattorini, D., et al., 2014. A thermogenic hydrocarbon seep in shallow Adriatic Sea (Italy): Gas origin, sediment contamination and benthic foraminifera. Mar. Petrol. Geol. 57, 283–293. https://doi.org/10.1016/j.marpetgeo.2014.06.006.

Galimov, E.M., 2006. Isotope organic geochemistry. Org. Geochem. 37, 1200–1262. https://doi.org/10.1016/j.orggeochem.2006.04.009.

Gao, L., He, P., Jin, Y., et al., 2016. Determination of position-specific carbon isotope ratios in propane from hydrocarbon gas mixtures. Chem. Geol. 435, 1–9. https://doi.org/10.1016/j.chemgeo.2016.04.019.

Gilbert, A., Sherwood Lollar, B., Musat, F., et al., 2019. Intramolecular isotopic evidence for bacterial oxidation of propane in subsurface natural gas reservoirs. Proc. Natl. Acad. Sci. 116, 6653–6658. https://doi.org/10.1073/pnas.1817784116.

Gilbert, A., Yamada, K., Suda, K., et al., 2016. Measurement of position-specific ^{13}C isotopic composition of propane at the nanomole level. Geochem. Cosmochim. Acta 177, 205–216. https://doi.org/10.1016/j.gca.2016.01.017.

Gold, T., Soter, S., 1980. Deep-earth-gas hypothesis. Sci. Am. 242, 130–137.

Guo, J., Chen, H., Su, Z., 2014. Sandboby development of taiyuan formation under central paleouplift, ordos Basin. Natural Gas Exp. Develop. 37, 5–8 (in Chinese).

Hao, F., Guo, T., Zhu, Y., et al., 2008. Evidence for multiplesta ges of oil cracking and thermochemical sulfate reduction in the Puguang gasfield, Sichuan Basin, China. Am. Assoc. Petrol. Geol. Bull. 5, 611–637. https://doi.org/10.1306/01210807090.

Hao, Y., Li, J., Wei, Z., et al., 2013. Molecular simulation on pyrolysis mechanism of butane. Acta Pet. Sin. 29, 824–829. https://doi.org/10.3969/j.issn.1001-8719.2013.05.013 (in Chinese).
He, D., Bao, H., Sun, F., et al., 2020. Geologic structure and genetic mechanism for the central uplift in the Ordos Basin. Chin. J. Geol. 55, 627–656. https://doi.org/10.12017/dzkx.2020.039 (in Chinese).
He, D., Bao, H., Kai, B., et al., 2021. Critical tectonic modification periods and its geologic features of Ordos Basin and adjacent area. Acta Pet. Sin. 42, 1255–1269. https://doi.org/10.7623/syxb202110001 (in Chinese).
He, D., Niu, X., Zheng, N., et al., 2024. Tectonic differentiation and distribution of early Paleozoic Ordos basin. Acta Geol. Sin. 98 (12), 3601-3618. https://doi.org/10.19762/j.cnki.dizhixuebao.2024432 (in Chinese).
Huang, J., Jing, X., Zhang, Y., et al., 2024. Geological characteristics and origin analysis of bitumen in Cambrian reservoirs of Ordos basin. Acta Geol. Sin. 98 (10), 3134-3148. https://doi.org/10.19762/j.cnki.dizhixuebao.2023297 (in Chinese).
Huang, J., Lin, J., Zhang, Y., et al., 2022. The organic geochemical characteristics of Lower Cambrian marine source rocks and its contribution to hydrocarbon accumulation in the southern margin of Ordos Basin. Nat. Gas Geosci. 33, 461–471. https://doi.org/10.11764/j.issn.1672-1926.2021.11.007 (in Chinese).
Huang, Z., Liang, T., Zhan, Z., et al., 2018. Chemical structure evolution of kerogen during oil generation. Mar. Petrol. Geol. 98, 422–436. https://doi.org/10.1016/j.marpetgeo.2018.08.039.
Jenden, P.D., Kaplan, I.R., Poreda, R., et al., 1988. Origin of nitrogen-rich natural gases in the California great valley: Evidence from helium, carbon and nitrogen isotopic ratios. Geochem. Cosmochim. Acta 52, 851–861. https://doi.org/10.1016/0016-7037(88)90356-0.
Jin, B., Peng, P., Jin, B., et al., 2024. Modeling position specific carbon isotopologue fractionation of thermogenic propane and precursors modeling position specific carbon isotopologue fractionation of thermogenic propane and precursors. Innov. Geosci., 100054 https://doi.org/10.59717/j.xinn-geo.2024.100054.
Li, E., Pan, C., Yu, S., et al., 2013. Hydrocarbon generation from coal, extracted coal and bitumen rich coal in confined pyrolysis experiments. Org. Geochem. 64, 58–75. https://doi.org/10.1016/j.orggeochem.2013.09.004.
Li, X., Mastalerz, M., Horita, J., 2022. Gas generation and intramolecular isotope study in laboratory pyrolysis of the Springfield coal from the Illinois Basin. Org. Geochem. 171, 104466. https://doi.org/10.1016/j.orggeochem.2022.104466.
Li, Y., Jiang, W., Liu, W., et al., 2024. Contribution of abiotic methane polymerization of C_{2+} hydrocarbons in highly mature natural gas reservoirs. Org. Geochem. 192, 104798. https://doi.org/10.1016/j.orggeochem.2024.104798.
Liu, B., Yan, D., Fu, X., et al., 2018. Technical papers investigation of geochemical characteristics of hydrocarbon gas and its implications for late Miocene transpressional strength - a study in the Fangzheng Basin, Northeast China. Interpretation 6, 1F–T229. https://doi.org/10.1190/INT-2017-0092.1.
Liu, C., Liu, P., McGovern, G.P., et al., 2019b. Molecular and intramolecular isotope geochemistry of natural gases from the Woodford Shale, Arkoma Basin, Oklahoma. Geochem. Cosmochim. Acta 255, 188–204. https://doi.org/10.1016/j.gca.2019.04.020.
Liu, C., Liu, P., Wang, X., et al., 2023b. Establishing accuracy of position-specific carbon isotope analysis of propane by GC-pyrolysis-GC-IRMS. Rapid Commun. Mass Spectrom. e9494. https://doi.org/10.1002/rcm.9494.
Liu, C., McGovern, G.P., Liu, P., et al., 2018b. Position-specific carbon and hydrogen isotopic compositions of propane from natural gases with quantitative NMR. Chem. Geol. 491, 14–26. https://doi.org/10.1016/j.chemgeo.2018.05.011.
Liu, P., Wang, X., Liu, C., et al., 2024. Intramolecular carbon isotopic rollover in propane from natural gas reservoirs of the Santanghu Basin: Insights into chemical structure of kerogen. Org. Geochem. 188, 104740. https://doi.org/10.1016/j.orggeochem.2024.104740.
Liu, P., Wang, X., Liu, C., et al., 2023a. Kinetic isotope effect and reaction pathways of thermogenic propane generation at early maturation stage: insights from position-specific carbon isotope distribution. Mar. Petrol. Geol. 153, 106252. https://doi.org/10.1016/j.marpetgeo.2023.106252.
Liu, P., Wang, X., Liu, H., Horita, J., Zhou, G., Bao, H., 2025a. Intramolecular carbon isotopic fractionation of propane via thermochemical sulfate reduction (TSR) in natural gas reservoirs. Nat. Gas Ind. B. 13 (1), 1–8. https://doi.org/10.1016/j.ngib.2025.12.001.
Liu, P., Wang, X., Wang, J., et al., 2025b. Deciphering origins of hydrocarbon deposits by means of intramolecular carbon isotopes of propane adsorbed on sediments. Pet. Sci. 22 (2), 546–556. https://doi.org/10.1016/j.petsci.2024.10.007.
Liu, Q., Dai, J., Jin, Z., et al., 2016. Abnormal carbon and hydrogen isotopes of alkane gases from the Qingshen gas field, Songliao Basin, China, suggesting abiogenic alkanes? J. Asian Earth Sci. 115, 285–297. https://doi.org/10.1016/j.jseaes.2015.10.005.
Liu, Q., Dai, J., Zhang, T., et al., 2007. Genetic types of natural gas and their distribution in Tarim Basin, NW China. J. Nat. Sci. Sustain. Technol. 1, 603–620.
Liu, Q., Jin, Z., Meng, Q., et al., 2015. Genetic types of natural gas and filling patterns in Daniudi gas field, Ordos Basin, China. J. Asian Earth Sci. 107, 1–11. https://doi.org/10.1016/j.jseaes.2015.04.001.
Liu, Q., Jin, Z., Wang, X., et al., 2018c. Distinguishing kerogen and oil cracked shale gas using H, C-isotopic fractionation of alkane gases. Mar. Petrol. Geol. 91, 350–362. https://doi.org/10.1016/j.marpetgeo.2018.01.006.
Liu, Q., Wu, X., Wang, X., et al., 2019a. Carbon and hydrogen isotopes of methane, ethane, and propane: a review of genetic identification of natural gas. Earth Sci. Rev. 190, 247–272. https://doi.org/10.1016/j.earscirev.2018.11.017.
Liu, Q., Jin, Z., Li, H., et al., 2018a. Geochemistry characteristics and genetic types of natural gas in central part of the Tarim Basin, NW China. Mar. Petrol. Geol. 89, 91–105. https://doi.org/10.1016/j.marpetgeo.2017.05.002.
Liu, R., 2015. Typical features of the first giant shale gasfield in China. Nat. Gas Geosci. 26, 1488-1498 (in Chinese).
Liu, W., Zhang, D., Wang, X., et al., 2004. Geochemistry study on gas-source correlation of natural gas. Acta Sedimentol. Sin. 27–32. https://doi.org/10.14027/i.cnki.cjxb.2004.s1.004 (in Chinese).
Liu, X., Wei, L., Liu, B., et al., 2021. Characteristics of natural gas accumulation in the Cambrian weathering crust in the southwestern Ordos Basin. Nat. Gas. Ind. 41, 13–21. https://doi.org/10.3787/j.issn.1000-0976.2021.04.002 (in Chinese).
Muscio, G.P.A., Horsfield, B., 1996. Neoformation of inert carbon during the natural maturation of a marine source rock: Bakken shale, Williston basin. Energy & Fuels 10, 10–18. https://doi.org/10.1021/ef950189d.
Peng, H., Wang, J., Liu, C., et al., 2023. Long-term and multiple stage exhumation of the Ordos Basin, western North China Craton: insights from seismic reflection, borehole and geochronological data. Earth Sci. Rev. 238, 104349. https://doi.org/10.1016/j.earscirev.2023.104349.
Peng, W., Liu, Q., Hu, Y., et al., 2020. A new interpretation of carbon isotope series reverse of highly-over mature alkane gases: Demethylation of Aromatic Hydrocarbons. Earth Sci. 45, 1308–1314. https://doi.org/10.3799/dqkx.2019.133 (in Chinese).
Piasecki, A., Sessions, A., Lawson, M., et al., 2018. Position-specific ^{13}C distributions within propane from experiments and natural gas samples. Geochem. Cosmochim. Acta. 220, 110–124. https://doi.org/10.1016/j.gca.2017.09.042.
Rooney, M.A., Claypool, G.E., Chung, H.M., 1995. Modeling thermogenic gas generation using carbon isotope ratios of natural gas hydrocarbons. Chem. Geol. 126, 219–232. https://doi.org/10.1016/0009-2541(95)00119-0.
Schoell, M., 1980. The hydrogen and carbon isotopic composition of methane from natural gases of various origins. Geochem. Cosmochim. Acta 44, 649–661. https://doi.org/10.1016/0016-7037(80)90155-6.
Schoell, M., 1983. Genetic characterization of natural gas. AAPG Bull. 67, 2225–2238. https://doi.org/10.1306/AD46094A-16F7-11D7-8645000102C1865D.
Sherwood, L.B., Lacrampe-Couloume, G., Slater, G.F., et al., 2006. Unraveling abiogenic and biogenic sources of methane in the Earth's deep subsurface. Chem. Geol. 226, 328–339. https://doi.org/10.1016/j.chemgeo.2005.09.027.
Sherwood, L.B., Westgate, T.D., Ward, J.A., et al., 2002. Abiogenic formation of alkanes in the Earth's crust is a minor source of global hydrocarbon reservoirs. Nature 416, 522. https://doi.org/10.1038/416522a.
Shuai, Y., Xiong, Y., Li, J., et al., 2023. Unusual 13C depletion in the central carbon of propane in the gases of Longmaxi shale in the Sichuan Basin. Org. Geochem. 184, 104658. https://doi.org/10.1016/j.orggeochem.2023.104658.
Song, D., Wu, C., Tuo, J., et al., 2021. Evolution of carbon isotopic compositions for gas generated in semi-closed pyrolysis system: Reflections on the formation of isotopic abnormal gases. J. Pet. Sci. Eng. 201, 108516. https://doi.org/10.1016/j.petrol.2021.108516.
Sun, L., Zhao, J., Li, J., et al., 2015. Hydrocarbon accumulation patterns of the upper Paleozoic gas in the longdong area, rdos Basin. Nat. Gas Geosci. 26, 2029–2038. https://doi.org/10.11764/j.issn.1672-1926.2015.11.2029 (in Chinese).
Sun, Y., Huang, C., 2004. Genesis characteristics and exploration significance of biogenic gas in Fangzheng rift. In: The Eighth Session of Ancient Geography and Sedimentological Abstracts of Academic Conference, vol. 88 (in Chinese).
Tilley, B., Muehlenbachs, K., 2013. Isotope reversals and universal stages and trends of gas maturation in sealed, self-contained petroleum systems. Chem. Geol. 339, 194–204. https://doi.org/10.1016/j.chemgeo.2012.08.002.
Wang, X., Li, X., Wang, X., et al., 2015a. Carbon isotopic fractionation by desorption of shale gases. Mar. Petrol. Geol. 60, 79–86. https://doi.org/10.1016/j.orggeochem.2015.03.010.
Wang, X., Liu, P., Liu, W., et al., 2024. Intramolecular carbon isotope of propane from coal-derived gas reservoirs of sedimentary basins: implications for source, generation and post-generation of hydrocarbons. Geosci. Front. 15, 101806. https://doi.org/10.1016/j.gsf.2024.101806.
Wang, X., Liu, W., Shi, B., et al., 2015b. Hydrogen isotope characteristics of thermogenic methane in Chinese sedimentary basins. Org. Geochem. 83–84, 178–189. https://doi.org/10.1016/j.orggeochem.2015.03.010.
Wang, X., Liu, W., Xu, Y., et al., 2006. The hydrogen isotopic composition of natural Gases generated from different pathways. Nat. Gas Geosci. 17, 163–169 (in Chinese).
Welhan, J.A., Craig, H., 1979. Methane and hydrogen in East Pacific rise hydrothermal fluids. Geophys. Res. Lett. 6, 829–831. https://doi.org/10.1029/GL006i011p00829.
Whiticar, M.J., 1999. Carbon and hydrogen isotope systematics of bacterial formation and oxidation of methane. Chem. Geol. 161, 291–314. https://doi.org/10.1016/S0009-2541(99)00092-3.
Xia, X., Chen, J., Braun, R., et al., 2013. Isotopic reversals with respect to maturity trends due to mixing of primary and secondary products in source rocks. Chem. Geol. 339, 205–212. https://doi.org/10.1016/j.chemgeo.2012.07.025.
Xia, X., Gao, Y., 2024. Compound-specific, intra-molecular, and clumped ^{13}C fractionations in the thermal generation and decomposition of ethane and propane: A DFT and ainetic investigation. Geochem. Cosmochim. Acta 375, 50–63. https://doi.org/10.1016/j.gca.2024.05.001.
Xu, Y., 1994. Genetic Theories of Natural Gases and their Application. Science Press, Beijing (in Chinese).
Xu, Y., Liu, W., Shen, P., et al., 2006. Carbon and hydrogen isotopic characteristics of natural gases from the Luliang and Baoshan basins in Yunnan Province, China. Sci. China Earth Sci. 49, 938–946. https://doi.org/10.1007/s11430-006-0938-8.

Yu, Z., Fan, L., Ren, J., et al., 2024. Natural gas accumulation models and favorable exploration areas of the Cambrian-Ordovician in the Ordos Basin. Nat. Gas. Ind. 44, 44–57. https://doi.org/10.3787/j.issn.1000-0976.2024.08.004 (in Chinese).

Zhang, L., Li, Y., Jiang, W., et al., 2022. Position-specific carbon isotopic composition of thermogenic propane: Insights from pyrolysis experiments. Org. Geochem. 166, 104379. https://doi.org/10.1016/j.orggeochem.2022.104379.

Zhang, M., Song, D., Wang, T., et al., 2023. Comparative study and its significance of geochemical characteristics of source rocks from Shanxi Formation and Taiyuan Formation in Hangingi area of Ordos Basin. J. Yangtze Univ. (Natural Sci. Ed.) 20, 55–66. https://doi.org/10.16772/j.cnki.1673-1409.2023.05.001 (in Chinese).

Zhang, T., Sun, X., Milliken, K.L., et al., 2017. Empirical relationship between gas composition and thermal maturity in Eagle Ford Shale, south Texas. AAPG Bull. 101 (8), 1277–1307. https://doi.org/10.1306/09221615209.

Zhao, H., Liu, C., Larson, T.E., et al., 2020. Bulk and position-specific isotope geochemistry of natural gases from the Late Cretaceous Eagle Ford Shale, south Texas. Mar. Petrol. Geol. 122, 104659. https://doi.org/10.1016/j.marpetgeo.2020.104659.

Zhao, H., Liu, C., Wang, F., et al., 2016. Structural division and characteristics in the western edge of Ordos Basin. Oil Gas Geol. 27, 173–179 (in Chinese).

Zumberge, J., Ferworn, K., Brown, S., 2012. Isotopic reversal ('rollover') in shale gases produced from the Mississippian Barnett and Fayetteville formations. Mar. Petrol. Geol. 31, 43–52. https://doi.org/10.1016/j.marpetgeo.2011.06.009.